

1

## **Supplementary Information**

2

**Melatonin ameliorates necrotizing enterocolitis by preventing Th17/Treg imbalance**

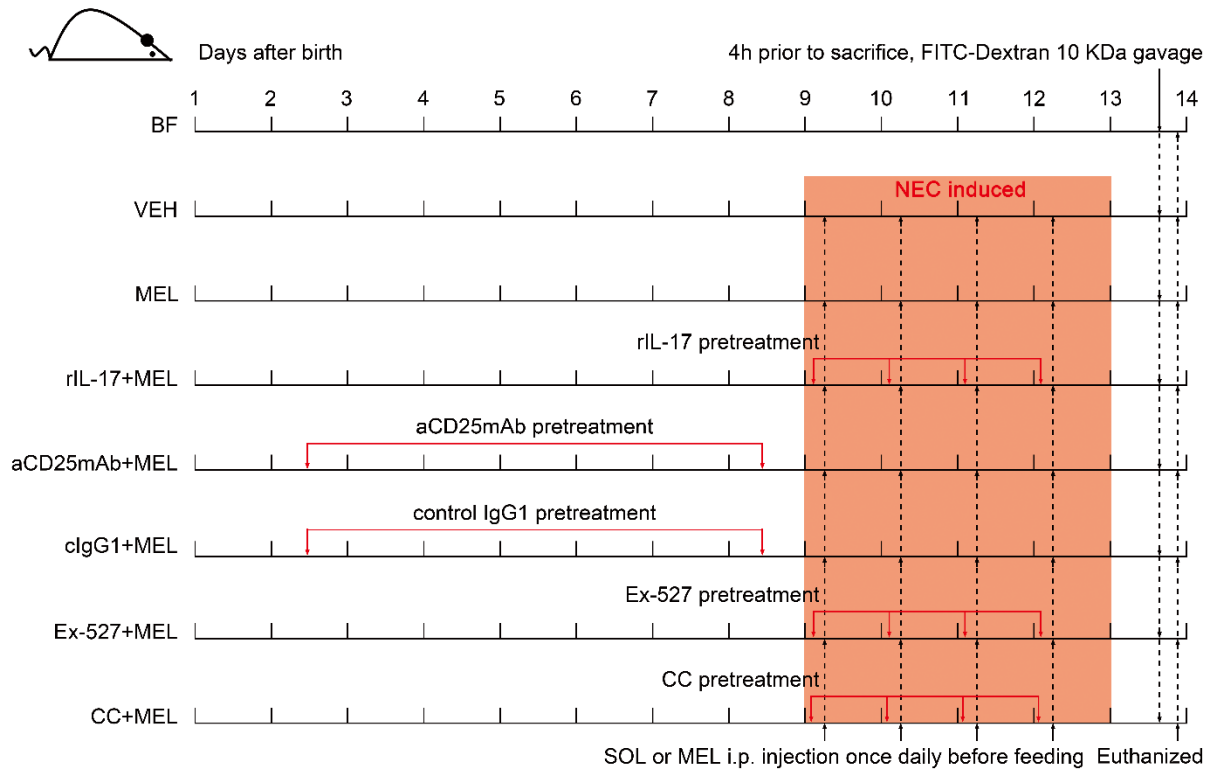
3

**through activation of the AMPK/SIRT1 pathway**

4

Ma et al.

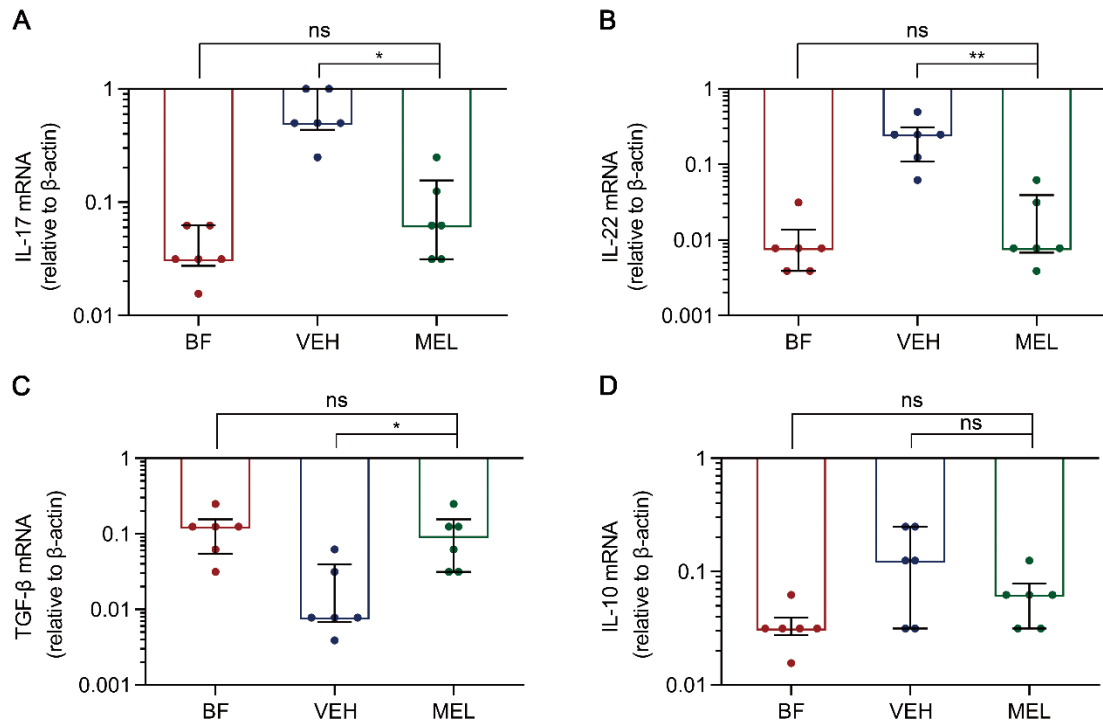
5



6

7 **Supplementary Figure 1. Diagrammatic representation of the experimental models.**

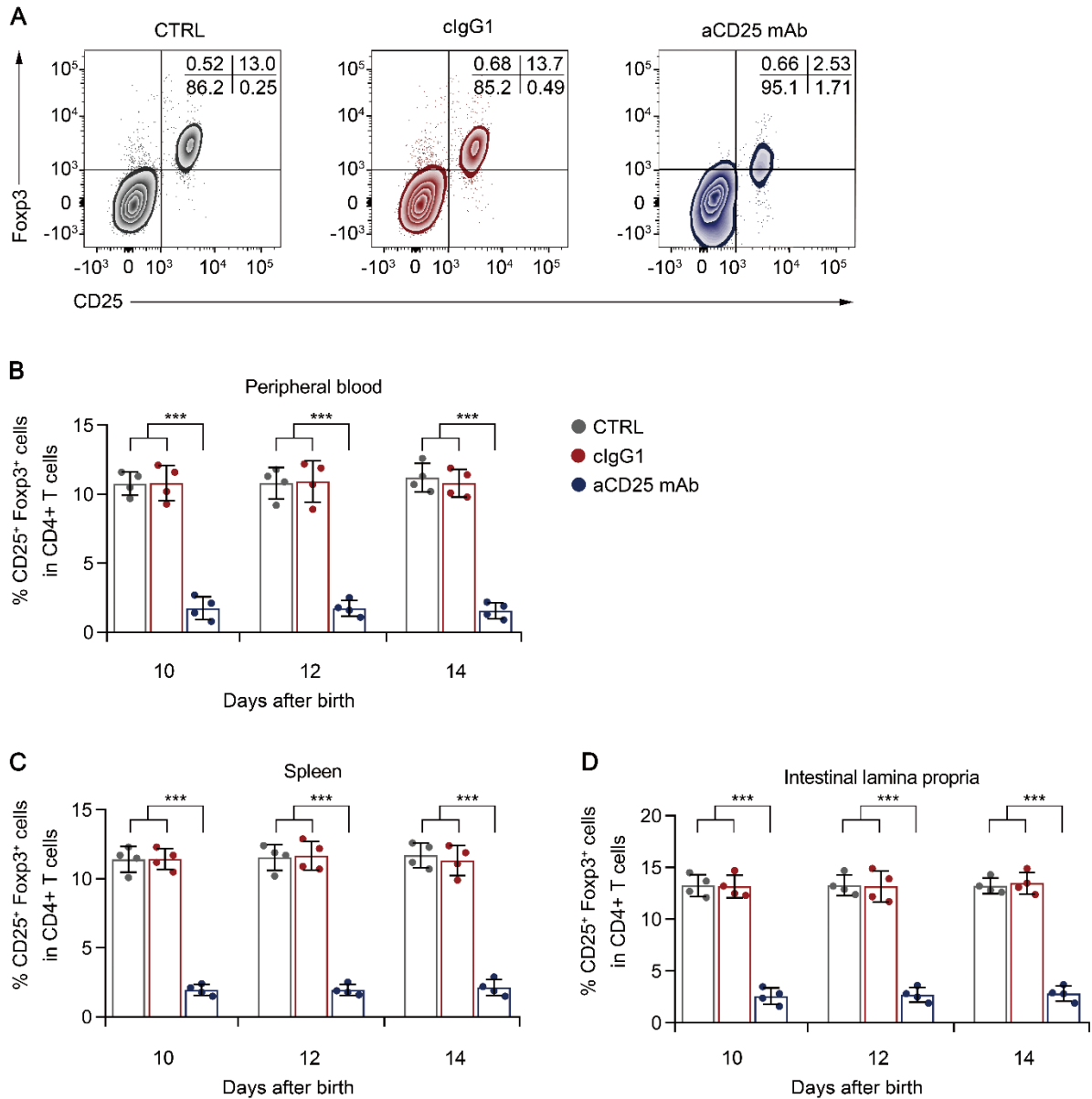
8 Schematic shows the specific role of melatonin in a mouse necrotizing enterocolitis (NEC)  
 9 model (melatonin group, MEL), melatonin combined with rIL-17 (melatonin + rIL-17 group,  
 10 MEL + rIL-17), melatonin combined with aCD25 mAb (melatonin+ aCD25 mAb group,  
 11 MEL+ aCD25 mAb), melatonin combined Ex-527 (melatonin + Ex-527 group, MEL+  
 12 Ex-527), and melatonin combined Compound C (melatonin + Compound C group, MEL+  
 13 CC). Naïve control mice (BF group) were observed over the study period without intervention  
 14 and left with their dams to breastfeed. Simultaneously, controls also included the experimental  
 15 pups, which were treated only with a vehicle (consisting of < 25% ethanol in PBS, VEH  
 16 group) or melatonin combined with control IgG1 (melatonin + cIgG1 group, MEL+ cIgG1) at  
 17 the indicated time points.



18

19 **Supplementary Figure 2.** (A–D) Real-time qRT-PCR analysis of relative mRNA  
 20 expression of *IL-17* (A), *IL-22* (B), *TGF- $\beta$*  (C) and *IL-10* (D) in ileum of breastfed (BF group)  
 21 and NEC pups upon melatonin treatment (MEL group) or treatment with vehicle (consisting  
 22 of < 25% ethanol in PBS, VEH group). Each symbol (A–D) represents an individual  
 23 experiment (n = 6); column graphs represent the median with interquartile range, \* $P < 0.05$ ;  
 24 \*\* $P < 0.01$ ; ns: not significant.  $P$  values were calculated using Kruskal-Wallis followed by the  
 25 Pairwise Comparison test (A–D).

26

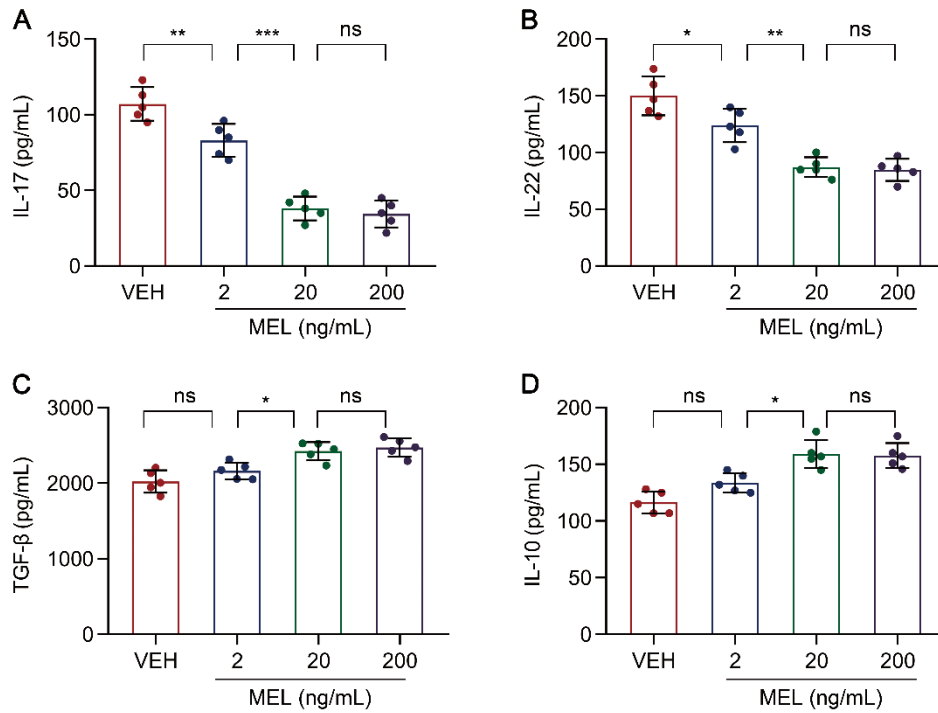


27

28 **Supplementary Figure 3. Anti-CD25 monoclonal antibody (aCD25 mAb) depletes CD4<sup>+</sup>**  
 29 **CD25<sup>+</sup> Fcγp3<sup>+</sup> Treg cells.** (A) Representative flow cytometry plots of CD25 and Fcγp3  
 30 expression in gated peripheral blood CD4<sup>+</sup> T cells from breastfed (CTRL group) and pups  
 31 upon aCD25 mAb treatment (aCD25 mAb group) or treatment with control IgG1 antibody  
 32 (clgG1 group) on day 2 and 8 after birth. (B–D) Quantification of the percentages of Treg  
 33 cells in the peripheral blood (B), spleen (C) and intestinal lamina propria (D) on day 10, 12,

34 and 14 after birth. Each symbol (**B–D**) represents an individual mouse ( $n = 4$ ); column graphs  
35 represent the mean with error bars indicating standard deviation (SD),  $***P < 0.001$ .  $P$  values  
36 were derived through one-way ANOVA followed by the Bonferroni multiple comparison test  
37 (**B–D**). Data are representative of two independent experiments (**B–D**).

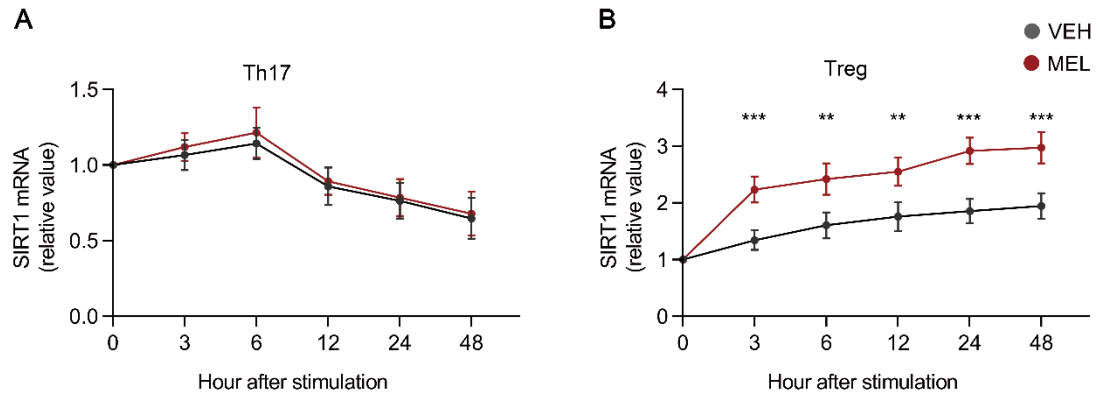
38



39

40 **Supplementary Figure 4.** (A–D) The concentrations of IL-17 (A), IL-22 (B), TGF-β (C),  
 41 and IL-10 (D) in the culture supernatants of Th17 (A, B) and Treg (C, D) conditions, in the  
 42 presence of melatonin at different concentrations (0 to 200 ng/mL) (as described in Methods).  
 43 Each symbol (A–D) represents an individual experiment (n = 5); column graphs represent the  
 44 mean with error bars indicating standard deviation (SD), \* $P < 0.05$ ; \*\* $P < 0.01$ ; \*\*\* $P < 0.001$ ;  
 45 ns: not significant.  $P$  values were derived through one-way ANOVA followed by the  
 46 Bonferroni multiple comparison test (A–D).

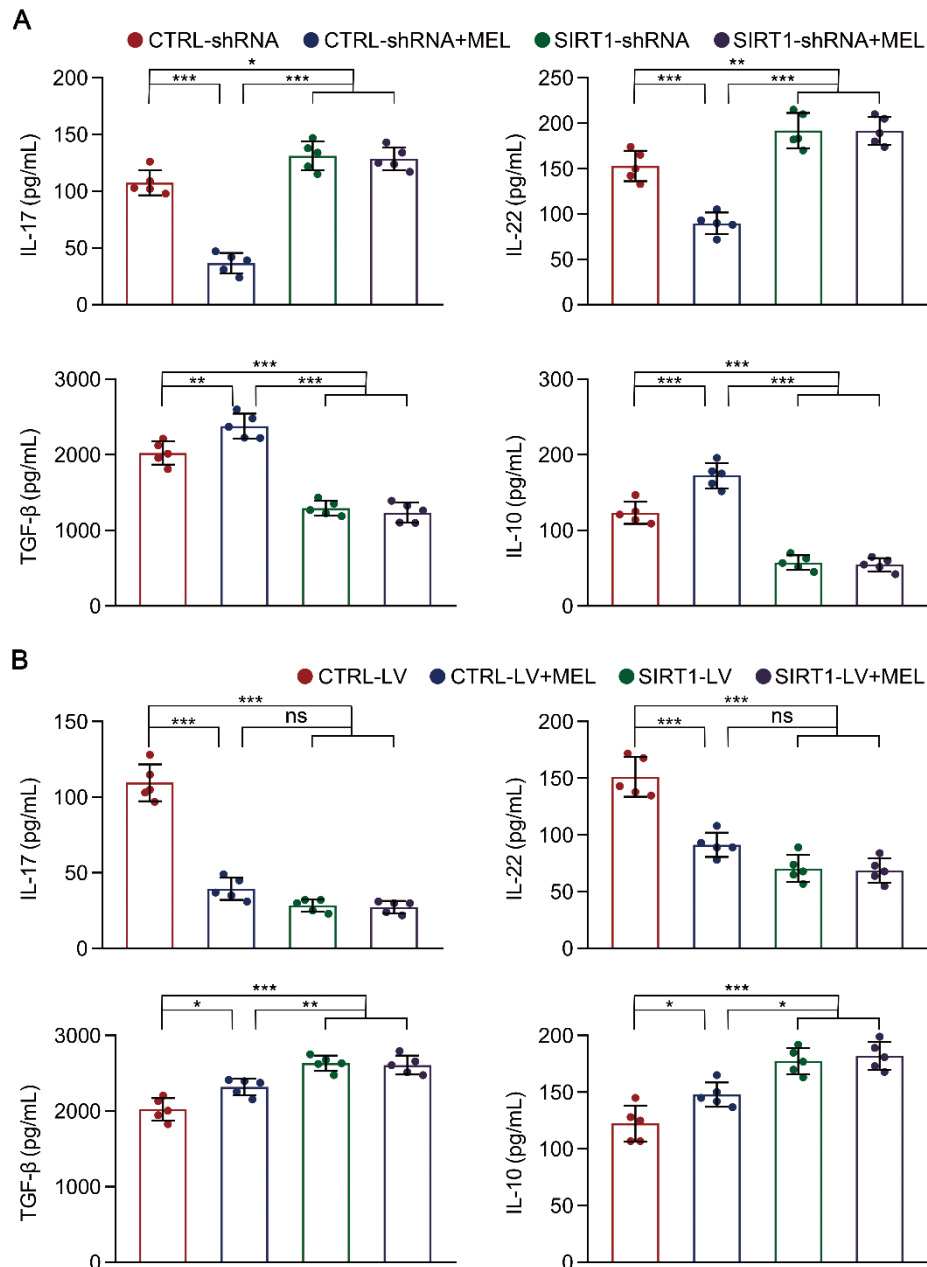
47



48

49 **Supplementary Figure 5.** *SIRT1* mRNA expression as examined by Real-time qRT-PCR  
 50 analysis in naïve CD4<sup>+</sup> T cells of umbilical cord blood from healthy newborns were activated  
 51 under Th17 (A) or Treg (B) conditions for different time courses, in the presence of melatonin  
 52 (20 ng/ml) (MEL group) or vehicle (consisting of < 25% ethanol in PBS, VEH group). Data  
 53 are shown as the mean with error bars indicating standard deviation (SD), n = 4. \*\*P<0.01  
 54 and \*\*\*P<0.001. P values were calculated using the nonparametric Student's *t*-tests.

55

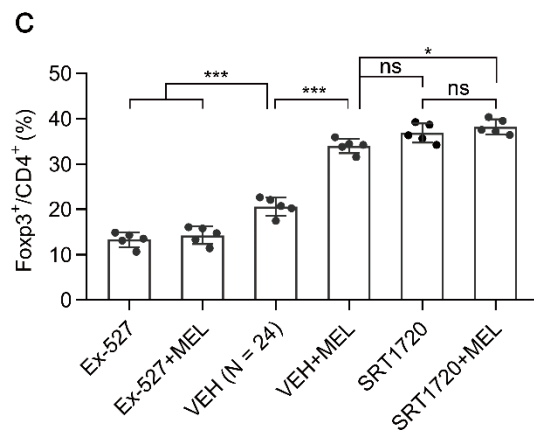
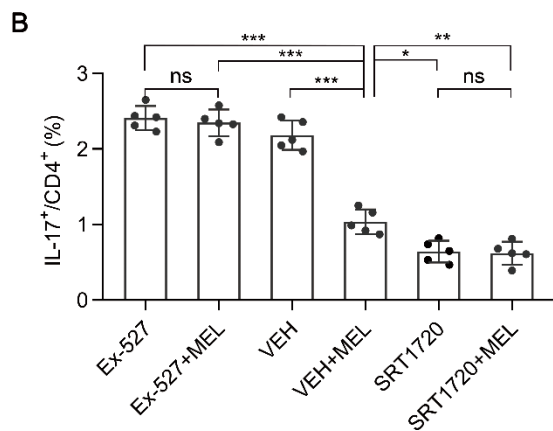
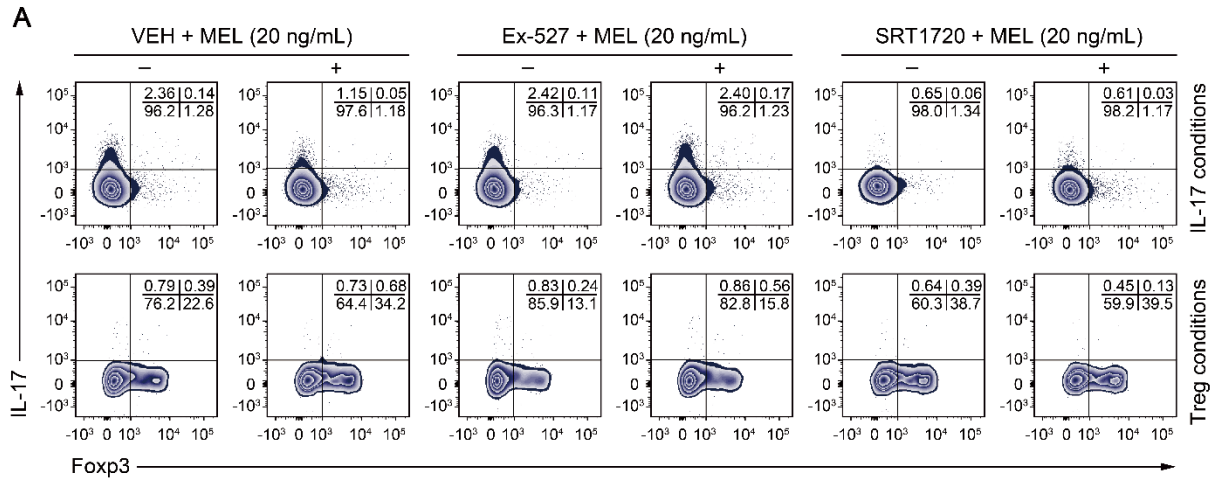


56

57 **Supplementary Figure 6.** Sorted naïve CD4<sup>+</sup> T cells from umbilical cord blood of healthy  
 58 newborns were transduced with lentivirus-containing control-shRNA (CTRL shRNA) and  
 59 SIRT1-shRNA (SIRT1 shRNA) (A), or control lentivirus (CTRL LV), and SIRT1-expressing  
 60 lentivirus (SIRT1 LV) (B). At 24 h after transduction, CD4<sup>+</sup> T cells were differentiated under  
 61 Th17 or Treg conditions for four days, in the presence of melatonin (20 ng/mL). Then the  
 62 culture supernatants were collected and IL-17, IL-22, TGF-β, and IL-10 levels in the



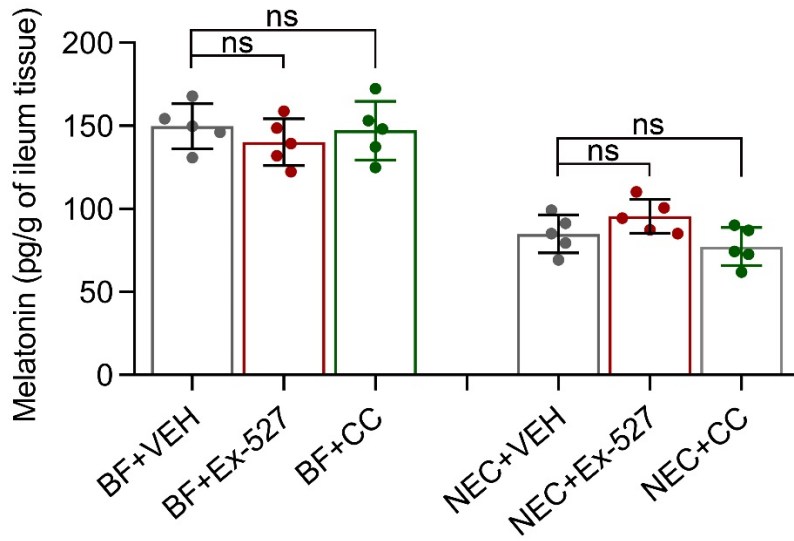
63 supernatants were monitored by ELISA. Each symbol (**A**, **B**) represents an individual  
64 experiment (n = 5); column graphs represent the mean with error bars indicating standard  
65 deviation (SD), \* $P < 0.05$ ; \*\* $P < 0.01$ ; \*\*\* $P < 0.001$ ; ns: not significant.  $P$  values were  
66 derived through one-way ANOVA followed by the Bonferroni multiple comparison test (**A**,  
67 **B**).  
68



69

70 **Supplementary Figure 7.** Sorted naïve CD4<sup>+</sup> T cells of umbilical cord blood from healthy  
 71 newborns were differentiated under Th17 or Treg conditions for 5 days, in the presence of  
 72 vehicle (0.01% DMSO, VEH), melatonin (MEL), Ex-527, Ex-527+MEL, SRT1720, or  
 73 SRT1720+MEL. Melatonin, Ex-527 (10  $\mu$ M), SRT1720 (1  $\mu$ M) and vehicle were added at the  
 74 start of the cultures and at day 2. **(A)** Representative flow cytometry plots of IL-17 and Foxp3  
 75 expression in gated CD4<sup>+</sup> T cells under Th17 (top) and Treg (bottom) conditions. **(B, C)**  
 76 Quantification of the frequency of Th17 **(B)** and Treg **(C)** cells in **(A)**. Each symbol **(B, C)**  
 77 represents an individual experiment (n = 5); column graphs represent the mean with error bars  
 78 indicating standard deviation (SD), \* $P < 0.05$ ; \*\* $P < 0.01$ ; \*\*\* $P < 0.001$ ; ns: not significant.

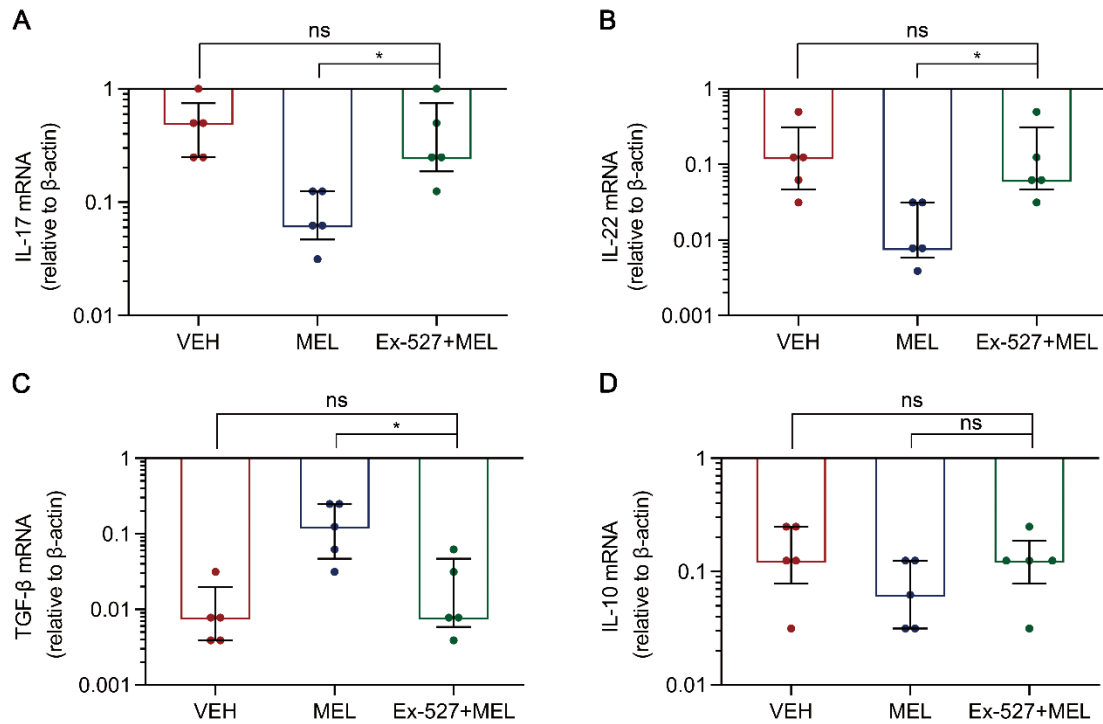
79 *P* values were derived through one-way ANOVA followed by the Bonferroni multiple  
80 comparison test (**B, C**).  
81



82

83 **Supplementary Figure 8.** ELISA analysis of the levels of melatonin in the small intestine  
 84 of breastfed (BF) and necrotizing enterocolitis (NEC) pups with Ex-527, Compound C (CC)  
 85 or vehicle (consisting of < 25% ethanol in PBS, VEH) treatment. Each symbol represents an  
 86 individual experiment (n = 5); column graphs represent the mean with error bars indicating  
 87 standard deviation (SD), ns: not significant. *P* values were derived through one-way ANOVA  
 88 followed by the Bonferroni multiple comparison test.

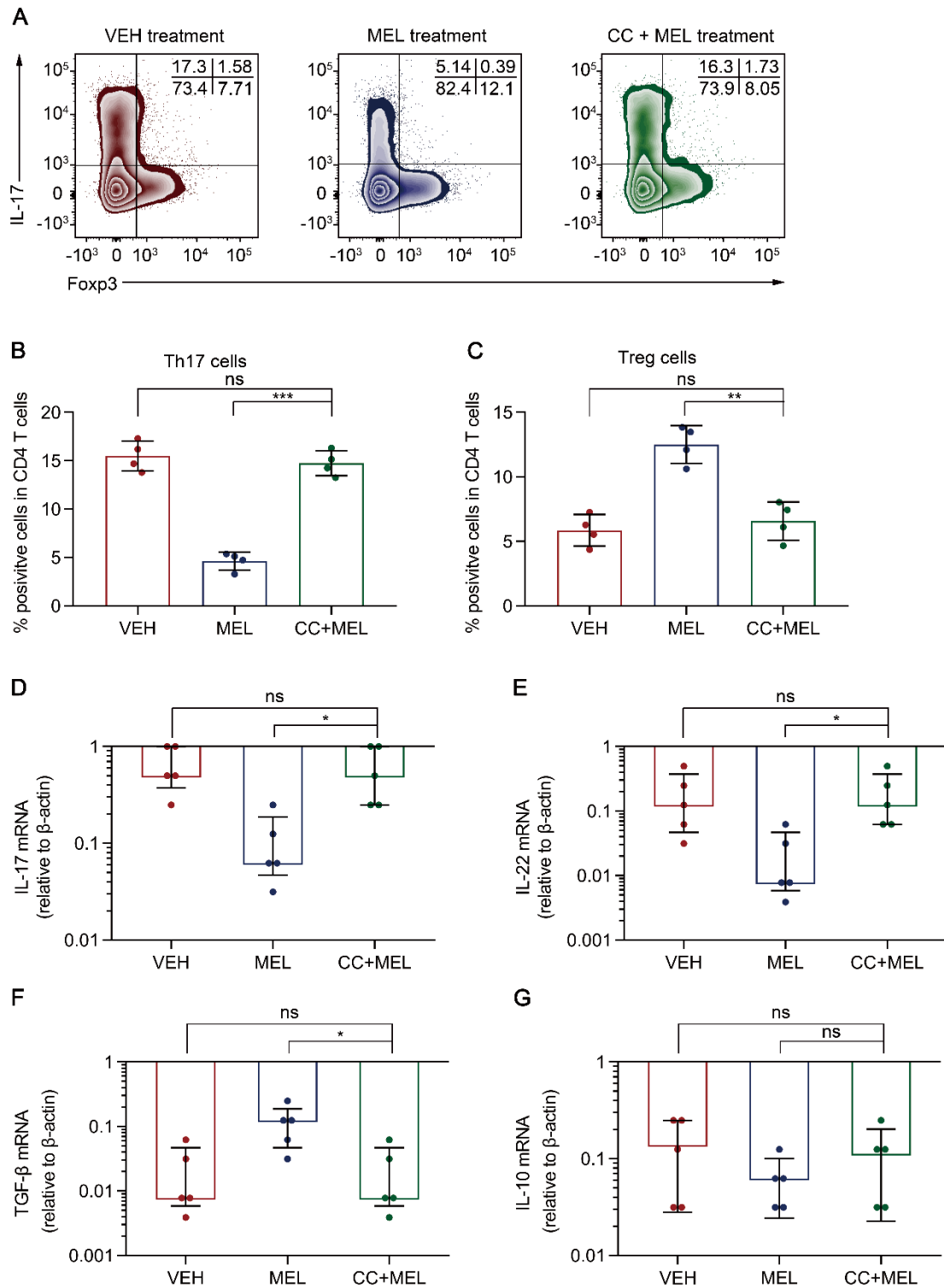
89



90

91 **Supplementary Figure 9.** (A–D) Real-time qRT-PCR analysis of relative mRNA  
 92 expression of *IL-17* (A), *IL-22* (B), *TGF- $\beta$*  (C) and *IL-10* (D) in ileum of NEC pups upon  
 93 vehicle (consisting of < 25% ethanol in PBS, VEH) treatment, or treatment with melatonin  
 94 (MEL) or melatonin combined with Ex-527 (MEL+Ex-527). Each symbol (A–D) represents  
 95 an individual experiment (n = 5); column graphs represent the median with interquartile range,  
 96 \* $P < 0.05$ ; ns: not significant.  $P$  values were derived through Kruskal-Wallis followed by the  
 97 Pairwise Comparisons test (A–D).

98

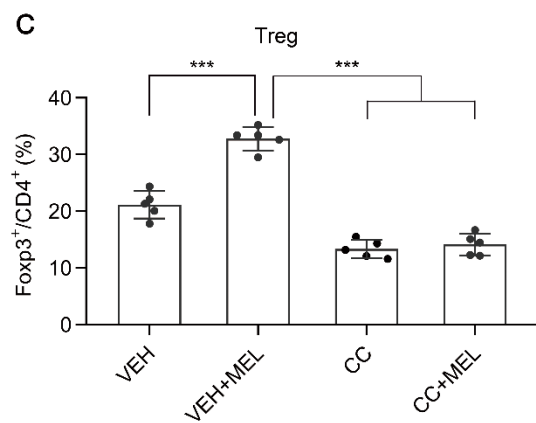
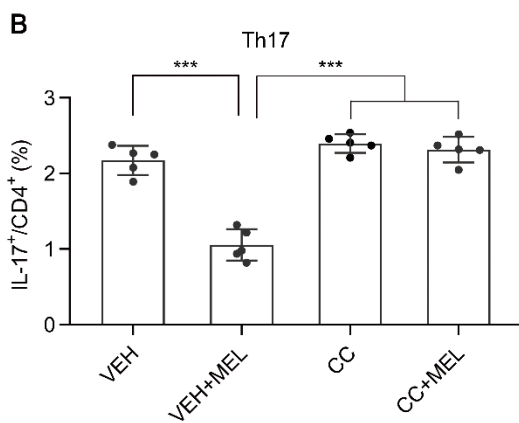
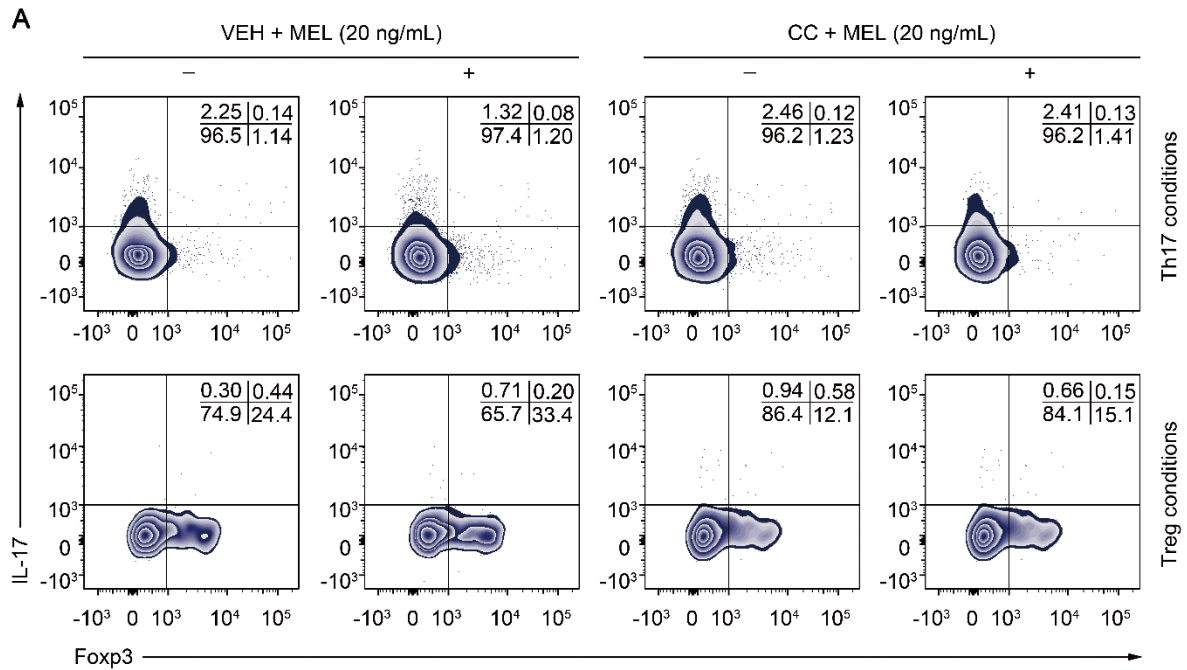


99

100 **Supplementary Figure 10. AMPK inhibition attenuates maintenance of the Th17/Treg**

101 **balance. (A) Representative flow cytometry plots of IL-17 and Foxp3 expression in gated**

102 lamina propria CD4<sup>+</sup> T cells from ileum sections of pups following NEC induction upon  
103 treatment with vehicle (VEH) alone or with melatonin (MEL) or melatonin combined with  
104 Compound C (MEL + CC). **(B, C)** Quantification of the percentages of Th17 **(B)** and Treg **(C)**  
105 cells in **(A)**, n = 4 per group. **(D–G)** Real-time qRT-PCR analysis of relative mRNA  
106 expression of *IL-17* **(D)**, *IL-22* **(E)**, *TGF-β* **(F)** and *IL-10* **(G)** in ileum of VEH (n = 5), MEL  
107 (n = 5), and MEL + CC (n = 5) groups. Each symbol **(B–G)** represents an individual  
108 experiment; column graphs represent the mean with error bars indicating standard deviation  
109 (SD) **(B, C)**, or median with interquartile range **(D–G)**, \**P* < 0.05; \*\**P* < 0.01; \*\*\**P* < 0.001;  
110 ns: not significant. *P* values were derived through one-way ANOVA followed by Bonferroni  
111 multiple comparison test **(B, C)** or Kruskal-Wallis followed by the Pairwise Comparisons test  
112 **(D–G)**.  
113



114

115 **Supplementary Figure 11.** Sorted naïve CD4<sup>+</sup> T cells of umbilical cord blood from healthy  
 116 newborns were differentiated under Th17 or Treg conditions for 5 days, in the presence of  
 117 vehicle (consisting of < 25% ethanol in PBS, VEH), melatonin (MEL), Compound C (CC), or  
 118 MEL + CC. Melatonin, Compound C (1 μM) and vehicle were added at the start of the  
 119 cultures and at day 2. (A) Representative flow cytometry plots of IL-17 and Foxp3 expression  
 120 in gated CD4<sup>+</sup> T cells under Th17 (top) and Treg (bottom) conditions. (B, C) Quantification of  
 121 the frequency of Th17 (B) and Treg (C) cells in (A). Each symbol (B, C) represents an



122 individual experiment ( $n = 5$ ); column graphs represent the mean with error bars indicating  
123 standard deviation (SD),  $***P < 0.001$ ; ns: not significant.  $P$  values were derived through  
124 one-way ANOVA followed by the Bonferroni multiple comparison test (**B, C**).

125

126 **Supplementary Table 1 Primers used for qRT-PCR in this study.**

Target gene	Primers
<b>Human</b>	
Foxp3	Forward: 5'-CGTGACAGTTTCCCACAAGC-3'
	Reverse: 5'-GGTGGCATGGGGTTCAAG-3'
ROR $\gamma$ t	Forward: 5'-GCTGGTTAGGATGTGCCG-3'
	Reverse: 5'-GAGTGGGAGAAGTCAAAGATGGA-3'
IL-10	Forward: 5'-ACCAAGACCCAGACATCAA-3'
	Reverse: 5'-CATTCTTCACCTGCTCCAC-3'
IL-17A	Forward: 5'-CTCGATTTACATGCCTTCA-3'
	Reverse: 5'-GAGGGGCCTTAATCTCCAAA-3'
IL-22	Forward: 5'-GAGGAATGTGCAAAAGCTGA-3'
	Reverse: 5'-GCTTTGGGGCATCTAATTGT-3'
TGF- $\beta$	Forward: 5'-CACGATCATGTTGGACAACCTGCTGC-3'
	Reverse: 5'-CTTCAGCTCCACAGAGAAGAAGCTGC-3'
SIRT1	Forward: 5'-GCAGATTAGTAGGCGGCTTG-3'
	Reverse: 5'-TCTGGCATGTCCCACACTATCA-3'
$\beta$ -actin	Forward: 5'-CCAGAGCAAGAGAGGCATCC-3'
	Reverse: 5'-TAGCACAGCCTGGATAGCAAC-3'
<b>Mouse</b>	
IL-10	Forward: 5'-TGGCCCAGAAATCAAGGAGG-3'
	Reverse: 5'-CAGCAGACTCAATACACACCT-3'
IL-17a	Forward: 5'-TTAACTCCCTTGGCGCAAAA-3'
	Reverse: 5'-CTTCCCTCCGCATTGACAC-3'
IL-22	Forward: 5'-CCGAGGAGTCAGTGCTAAGG-3'
	Reverse: 5'-TCTGGATGTTCTGGTCGTCA-3'
TGF- $\beta$	Forward: 5'-TGACGTCACCTGGAGTTGTACGG-3'

Reverse: 5'-GGTTCATGTCATGGATGGTGC-3'  
 Forward: 5'-AACTCCATCATGAAGTGTGA-3'  
 β-actin Reverse: 5'-ACTCCTGCTTGCTGATCCAC-3'

---

127 **Supplementary Table 2 Antibodies for flow cytometry.**

<b>Reagents</b>	<b>Clone</b>	<b>Manufacturer</b>
<b>Human</b>		
Anti-CD3-FITC	UCHT1	BD Biosciences
Anti-CD3-APC	UCHT1	BD Biosciences
Anti-CD4- FITC	RPA-T4	BD Biosciences
Anti-CD4- APC/Cy7	RPA-T4	BD Biosciences
Anti-CD25- PE-Cy7	M-A251	BD Biosciences
Anti-CD45RA- PE	5H9	BD Biosciences
Anti- FoxP3-PE	259D/C7	BD Biosciences
Anti- IL-17A- PerCP-Cy5.5	N49-653	BD Biosciences
<b>Mouse</b>		
Anti-CD3- FITC	17A2	BD Biosciences
Anti-CD4- APC/Cy7	GK1.5	BioLegend
Anti-CD25- PE-Cy7	3C7	BioLegend
Anti-Foxp3- PE	MF23	BD Biosciences
Anti- IL-17A- PerCP-Cy5.5	TC11-18H10	BD Biosciences